Inorganic Pyro-compounds $M_a[(X_2O_7)_b]$

By G. M. Clark
DEPARTMENT OF CHEMICAL SCIENCES, THE POLYTECHNIC, HUDDERSFIELD HD1 3DH

and R. Morley
NORTH-WEST FORENSIC SCIENCE LABORATORY, EUXTON, CHORLEY, LANCASHIRE

1 Introduction

Compounds of stoicheiometry $M_a[(X_2O_7)_b]$ exhibit an extraordinary variety of structural types. For example, $Ca_2Ta_2O_7$ is a complex oxide with the continuous framework structure of pyrochlorite.[1] $Y_2Pb_2O_7$ is similarly a continuous complex oxide but of the defect fluorite type, $(Y_2Pb_2)(\square O_7)$.[2] The compound $Na_2Mo_2O_7$, on the other hand, contains infinite one-dimensional chains $Mo_2O_7^{2-}$ within which Mo^{VI} atoms are both octahedrally and tetrahedrally co-ordinated.[3] $La_2Ge_2O_7$ is an example of a compound with the unusual B rare-earth disilicate structure containing both linear $Ge_3O_{10}^{8-}$ and tetrahedral GeO_4^{4-} anions.[4] Thortveitite, $Sc_2Si_2O_7$,[5] and lopezite, $K_2Cr_2O_7$,[6] are examples of compounds containing the diortho-anions $Si_2O_7^{6-}$ and $Cr_2O_7^{2-}$. These latter 'island' structures[7] containing discrete di- or pyro-anions are the subject of this review.

Crystal structures of compounds $M_a[(X_2O_7)_b]$, where $X_2O_7^{n-}$ is a discrete pyroanion, have been reported for X = As, Be, Cr, Ge, P, S, Si, and V. Other pyroanions probably exist, for example the i.r. spectrum of $K_2Se_2O_7$[8] has been interpreted in terms of the $Se_2O_7^{2-}$ anion, but no single-crystal *X*-ray determination has been reported for this species. In theory, a pyroanion $X_2O_7^{n-}$ may be formed by any atom X which is capable of tetrahedral co-ordination with oxygen. By simple ionic theory X can be any ion for which $r(^{IV}X^{n+})/r(^{II}O^{2-})$* is less than 0.414. Since $r(^{II}O^{2-})$ = 135 pm,[9] $r(^{IV}X^{n+})$ may take any value up to 55 pm. Of the structurally determined pyroanions the smallest X is $^{IV}S^{6+}$ (r = 12 pm) and the largest X is $^{IV}Ge^{4+}$ (r = 40 pm).

A wide range of cations M can be accommodated in structures containing the

* The Roman left superscript designates the co-ordination number.

[1] O. Knop, F. Brisse, and L. Sutarno, *Canad. J. Chem.*, 1965, **43**, 2812.
[2] W. E. Klee and G. Weitz, *J. Inorg. Nuclear Chem.*, 1969, **31**, 2367.
[3] I. Lindqvist, *Acta Chem. Scand.*, 1950, **4**, 1066.
[4] Yu. I. Smolin, Yu. F. Shepelev, and T. V Upatova, *Doklady Akad. Nauk S.S.S.R.*, 1969, **187**, 322.
[5] D. W J. Cruickshank, H. Lynton, and G. A. Barclay, *Acta Cryst.*, 1962, **15**, 491.
[6] E. A. Kuz'min, V. V. Ilyukhin, Yu. A. Kharitonov, and N. V. Belov, *Kristall Tech.*, 1969, **4**, 441; *Kristallografiya*, 1969, **14**, 788.
[7] G. Bergerhoff, *Angew. Chem. Internat. Edn.*, 1964, **3**, 686.
[8] R. G. Brown and S. D. Ross, *Spectrochim. Acta*, 1972, **28A**, 1263.
[9] R. D. Shannon and C. T Prewitt, *Acta Cryst.*, 1969, **B25**, 925.

pyro-group X_2O_7 but no compound in which $r(^{IV}X^{n+})$ exceeds $r(M)$ is known. The smallest $r(M)/r(^{IV}X^{n+})$ ratio yet found is that for $Cu_2V_2O_7$[$r(^{V}Cu^{2+})/r(^{IV}V^{5+})$ = 1.83; see Figure 1].

Any crystalline compound adopts the geometrical arrangement of its components (cations and pyroanions in this case) which enables its lattice energy to be maximized. In general, this occurs when the best compromise between attractive cation–anion interactions and repulsive anion–anion interactions is achieved. Maximum cation–anion attraction (the major component of the lattice energy) is achieved when the cation is spherically surrounded by anions. However, in $M_a[(X_2O_7)_b]$ compounds the pyroanion is a distinctly 'angular' species whose ability to approximate spherical shielding of the cations is enormously dependent on its own highly variable symmetry[10] (Figure 2). Crystal structures exceedingly sensitive to cation radii, cation polarizing powers, *etc.* are therefore to be expected, and a rich variety of $X_2O_7^{n-}$ packings has already been shown to exist. For example, over 25 different structures have already been reported for compounds of stoicheiometry $M_2X_2O_7$. Temperature-dependent polymorphism is also particularly common in these compounds; for example, at least four forms of $Rb_2Cr_2O_7$[11] and three forms of $Mg_2V_2O_7$[12,13] are known.

To date, over 80 single-crystal *X*-ray determinations (representing almost 50 different structures) have been reported for compounds containing $X_2O_7^{n-}$ pyroanions; 60 of these have been for the compounds $M_2X_2O_7$. In spite of this multitude of structures, only two major classes can be distinguished. These may be referred to as (i) thortveitite-like and (ii) dichromate-like. In the thortveitite-like structures the pyroanion is essentially in the staggered conformation (full D_{3d} symmetry in thortveitite itself), the X—O′—X angle at the bridging oxygen atom O′ is usually greater than 140° (180° in thortveitite itself) and O′ is not in the first co-ordination shell of any of the cations. In the dichromate-like structures the pyroanion is essentially eclipsed, the X—O′—X angle is usually less than 140°, and the bridging oxygen atom O′ is normally within the first co-ordination shell of at least one cation. Further, the eclipsed conformation is often stabilized by one cation bonding across both halves of the pyroanion.

No simple radius-ratio rule can be used to determine whether a given compound will adopt a thortveitite-like or a dichromate-like structure. However, Figure 1 shows that the line given by the simple expression $r(X) = 1.5\,r(M) - 110$ (values of r/pm) serves as a useful guide. Although all of the structural features associated with thortveitite-like and dichromate-like structures are normally to be found in any $M_a[(X_2O_7)_b]$ compound whose $r(X)$ and $r(M)$ places it to the left and to the right, respectively, of this line, a number of exceptions are found. For example, the structural features of $Co_2V_2O_7$[14] clearly place this compound in the dichromate-like class, although it distinctly occupies the

[10] R. W. Mooney, S. Z. Toma, and J. Brunvoll, *Spectrochim. Acta*, 1967, **23A**, 1541.
[11] Y. W. I. Vesnin and L. A. Khripin, *Zhur. neorg. Khim.*, 1966, **11**, 2216.
[12] G. M. Clark and R. Morley, *J. Solid State Chem.*, 1976, **16**, 429.
[13] R. Wollast and A. Tazairt, *Silicates Ind.*, 1969, **34**, 37.
[14] E. E. Sauerbrei, R. Faggiani, and C. Calvo, *Acta Cryst.*, 1974, **B30**, 2907.

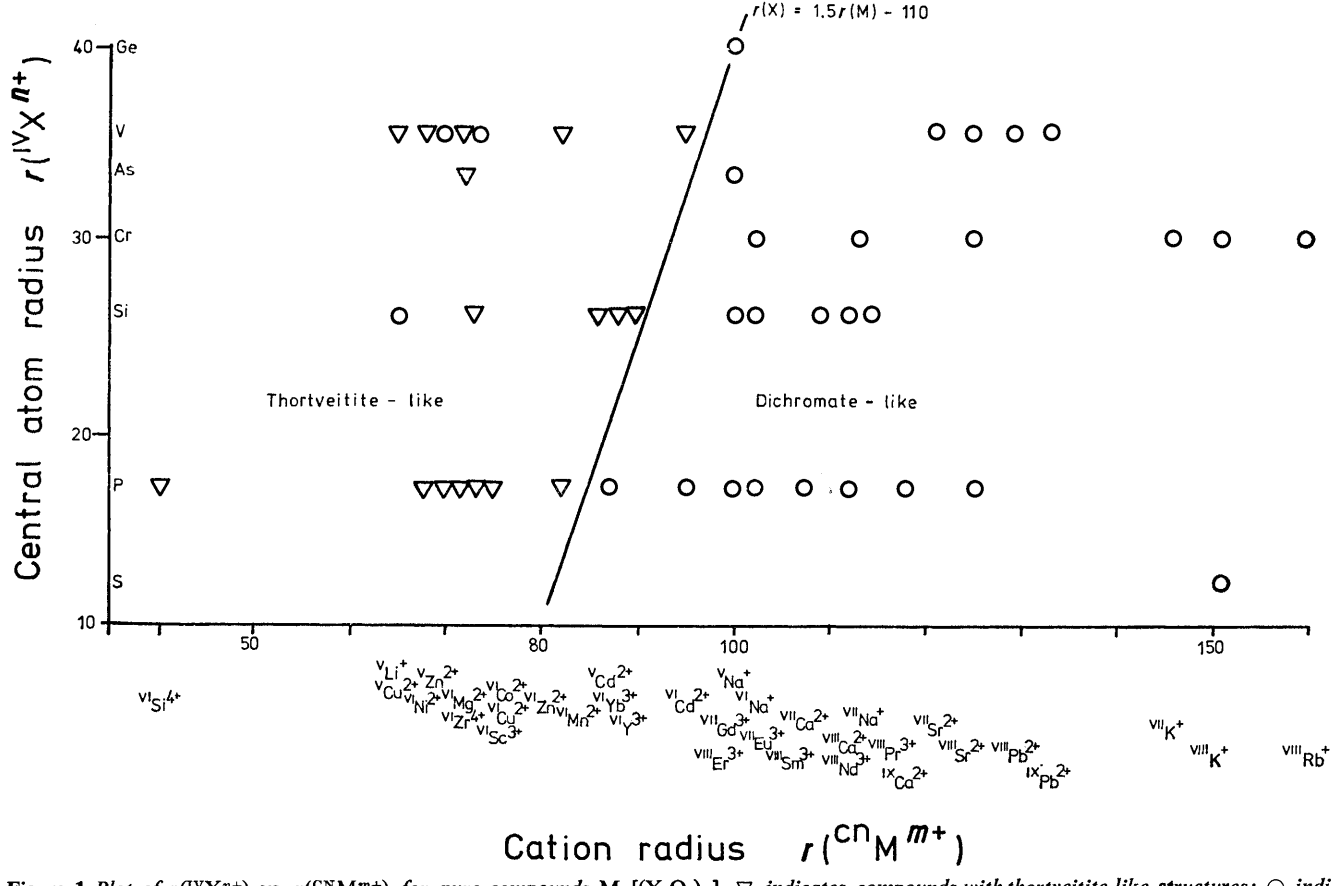

Figure 1 *Plot of* $r(^{IV}X^{n+})$ vs. $r(^{CN}M^{m+})$ *for pyro-compounds* $M_a[(X_2O_7)_b]$. ▽ *indicates compounds with thortveitite-like structures;* ○ *indicates compounds with dichromate-like structures (see text). Radii are those of Shannon and Prewitt,*[9] *values* /pm.

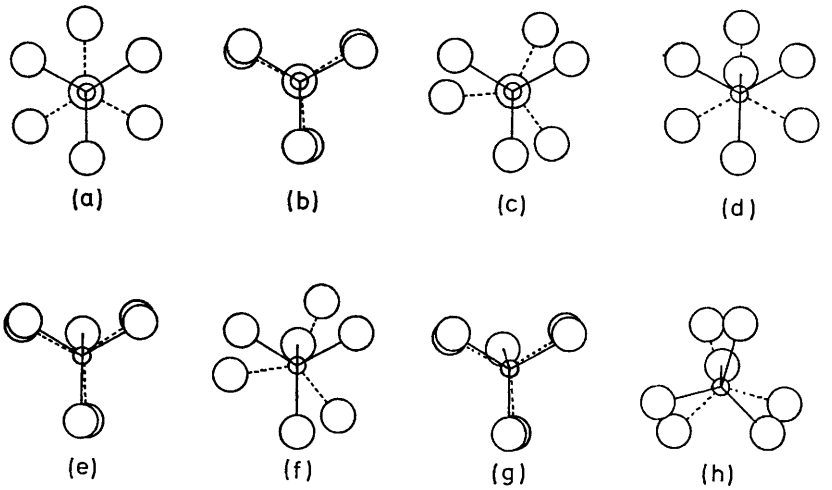

Figure 2 *Possible symmetries of* $X_2O_7^{n-}$ *pyroanions. (Only conformations with equivalent terminal* X—O *bonds and regular tetrahedral angles are illustrated).*
(a) D_{3d}, *(b)* D_{3h}, *(c)* D_3, *(d)* C_s, *(e)* C_{2v} *(syn- and anti-forms are possible), (f)* C_1, *(g)* C_s, *(h)* C_2.

thortveitite-like region in Figure 1. Similarly, the metastable (*C*2/*c*) form of $Rb_2Cr_2O_7$[15] is distinctly dichromate-like both in Figure 1 and in most of its structural features. However, the bridging atom O′ of the $Cr_2O_7^{2-}$ anion is 370 pm from the nearest Rb^+ ion, and there are eight nearest oxygen neighbours to each Rb^+ at distances between 289 and 314 pm. The sum of the ionic radii of $^{VIII}Rb^+$ and $^{II}O^{2-}$ is 295 pm,[9] therefore O′ cannot be considered as being within the first co-ordination shell of any cation, contrary to the normal situation in dichromate-like structures.

These few examples serve to emphasize that simple ionic theory, so useful to the understanding of stoicheiometrically simple compounds, cannot rationalize such factors as bridging angle and conformation. This can only be achieved in the light of more sophisticated models of bonding. It is the purpose of this review to present the various types of $M_a[(X_2O_7)_b]$ structures which have been elucidated and to indicate how progress towards an understanding of this complex branch of crystal chemistry is being made.

2 Dichromate-like Structures

A. Sheet Structures.—Brown and Calvo[16] have recently shown that the structures of some dichromate-like compounds of stoicheiometry $M_2X_2O_7$ are based on the stacking of centrosymmetric sheets of $X_2O_7^{n-}$ ion pairs. Sheets are

[15] P. Lofgren and K. Waltersson, *Acta Chem. Scand.*, 1971, **25**, 35.
[16] I. D. Brown and C. Calvo, *J. Solid State Chem.*, 1970, **1**, 173.

defined by two mutually perpendicular vectors ***B*** and ***C***, the former lying in the plane of the 'feet' of the pyroanions and making an angle of approximately 60° with their 'backbones' (see Figure 3). The approximately square sheets (***B*** ≈ ***C*** ≈

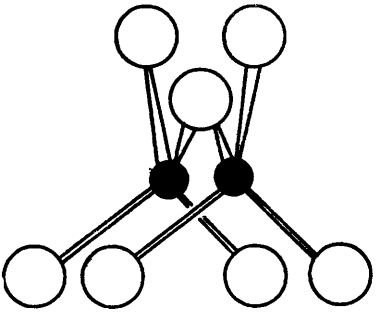

Figure 3 *The syn-C_{2v} conformation of the $X_2O_7^{n-}$ anion in dichromate-like structures. The 'feet' are the four O atoms of the base; the 'backbone' is formed by the three O atoms at the top.*

700 pm) may stack at 0°, 90°, 180°, or 270° to each other, and, being chiral, they may also stack so that sides of the same or sides of different chirality are in contact. Brown and Calvo[16] use the letter R to represent a sheet, so that the different stacking angles and chiralities are represented as in Table 1. Most dichromate-like structures are monoclinic or triclinic, with cell dimensions *a*, *b*, and *c* of approximately 750, 750, and 1300 pm, respectively. In such structures the ***B*** and ***C*** vectors approximate to the *yz* plane. For example, Figure 4 shows a drawing of the $P\bar{1}$ structure of $K_2Cr_2O_7$,[6,17–19] the Brown and Calvo [16] stacking sequence for which is R ⋈ R (Table 1). The first sheet, R, contains those K^+ ions and $Cr_2O_7^{2-}$ pyroanions cut by the *yz* (100) plane; the second sheet, ⋈, contains the ions cut by the (200) plane. These two sheets bear the relationship R ⋈ to each other since a rotation of one of them by 90° brings the two into mirror relationship. For simplicity of representation of dichromate-like structures and for ready comparison with the thortveitite-like structures, a projection on to the *xz* plane (occasionally *yz*) may be used. For example, the important features of the $P\bar{1}$ $K_2Cr_2O_7$ structure[6,17–19] (Figure 4) may be indicated as in Figure 5(b). Here the sheets defined by the vectors ***B*** and ***C*** are approximately normal to the page and lie in an approximately vertical direction.

By consideration of the different possible stacking orientations of sheets, at least ten different structures can be achieved. These are listed with known examples in Table 1. Although the formal differences are considerable, several pairs of these structures are closely related, and small displacements of atoms

[17] E. A. Kuz'min, V. V. Ilyukhin, and N. V. Belov, *Doklady Akad. Nauk S.S.S.R.*, 1967, **173**, 1068.
[18] J. K. Brandon and I. D. Brown, *Canad. J. Chem.*, 1968, **46**, 933.
[19] G. Brunton, *Materials Res. Bull.*, 1973, **8**, 271.

Table 1 *Sheet-type dichromate-like structures*

*Structure type**	*Examples*†	*Reference*	*Stacking sequence*
I	$Cd_2P_2O_7$	*a*	R R R
II			R ↺ R
III	β-$Ca_2P_2O_7$	*b*	§R ↷ R ↷ R
	β-$Sr_2V_2O_7$	*c*	
	A-$Sm_2Si_2O_7$	*d*	
	A-$Pr_2Si_2O_7$	*e*	
IV			§R ↷ R ↷ R
V	$P\bar{1}$-$K_2Cr_2O_7$	*f*	R ↷ R
VI	$Pb_2V_2O_7$	*g*	R ↻ R
VII	$P2_1/n$-$Rb_2Cr_2O_7$	*h*	‡R ↻ R
VIII	$P\bar{1}$-$Rb_2Cr_2O_7$	*i*	R ↻ R
IX			R ↷ R
X	$C2/c$-$Rb_2Cr_2O_7$	*j*	‡R ↻ R
	$(NH_4)_2Cr_2O_7$	*k*	
	$K_2S_2O_7$	*l*	

* After Brown and Calvo.[16] † Only compounds for which full single-crystal *X*-ray determinations have been reported are listed. Isotypes established by *X*-ray powder techniques are not included. ‡ VII and X differ only in the local symmetry of the sheets. Sheets of VII contain only a centre; sheets of X contain a centre, two-fold$_B$, and glide plane$_C$. § III and IV are enantiomorphic; $P4_1$ and $P4_3$ respectively.

[a] C. Calvo and P. K. L. Au, *Canad. J. Chem.*, 1969, **47**, 3409; [b] N. C. Webb, *Acta Cryst.*, 1966, **21**, 942; [c] J. A. Baglio and J. N. Dann, *J. Solid State Chem.*, 1972, **4**, 87; [d] Yu. I. Smolin and Yu. F. Shepelev, *Acta Cryst.*, 1970, **B26**, 484; [e] J. Felsche, *Z. Krist.*, 1971, **133**, 304; [f] J. K. Brandon and I. D. Brown, *Canad. J. Chem.*, 1968, **46**, 933; [g] R. D. Shannon and C. Calvo, *Canad. J. Chem.*, 1973, **51**, 70; [h] P. Lofgren, *Acta Chem. Scand.*, 1971, **25**, 44; [i] N. C. Panagiotopoulos and I. D. Brown, *Canad. J. Chem.*, 1970, **48**, 537; [j] P. Lofgren and K. Waltersson, *Acta Chem. Scand.*, 1971, **25**, 35; [k] G. A. P. Dalgaard, A. C. Hazell, and R. G. Hazell, *Acta Chem. Scand.* (*A*), 1974, **28**, 541; [l] H. Lynton and M. R. Truter, *J. Chem. Soc.*, 1960, 5112.

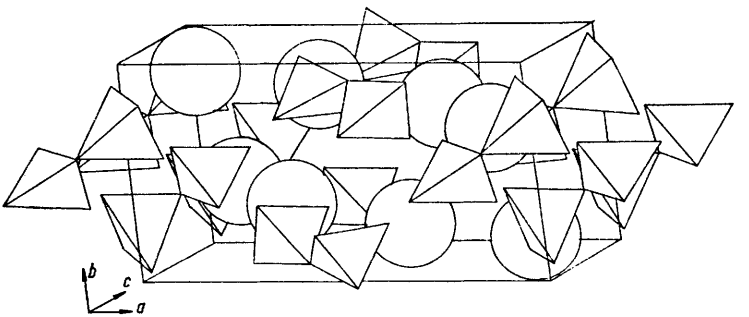

Figure 4 *The structure of* $K_2Cr_2O_7(P\bar{1})$. K^+ *ions are represented by open spheres,* $Cr_2O_7^{2-}$ *ions by corner-sharing tetrahedra.*

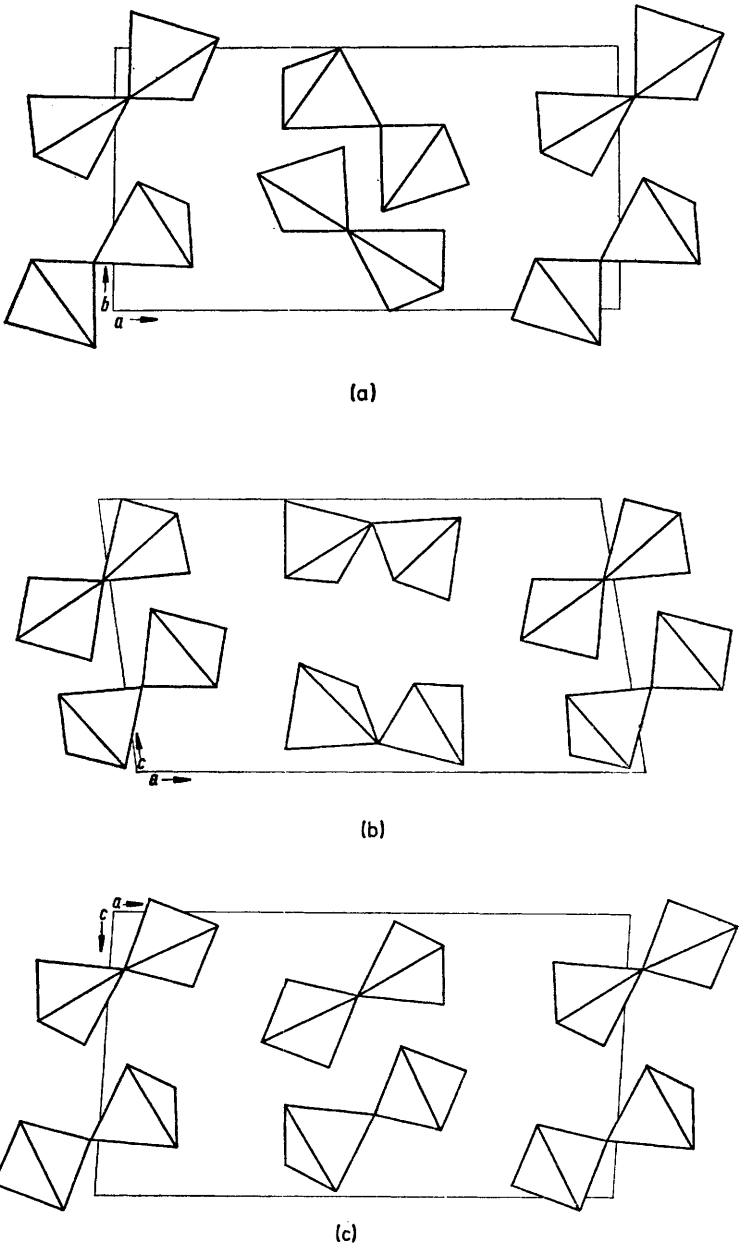

Figure 5 *Projections of some dichromate-like structures.* (*a*) *structure VI,* (*b*) *structure V,* (*c*) *structure VII.* (*See Table* 1).

are sufficient to cause interconversion. Polymorphic transitions between structures VI, V, VII, and X are particularly well established. Thus structure V is readily transformed into VI by a 90° anticlockwise rotation of the second sheet and into VII by a 90° clockwise rotation of the second sheet (see Figure 5). Also, since structure X differs little from VII (see note to Table 1), the sequence of transitions VI ↔ V ↔ VII ↔ X should be readily achieved. The rotatory relationship between the triclinic (V) and monoclinic (X) forms of $K_2Cr_2O_7$ was first noted by Kuz'min *et al.*,[6] who proposed that the formation of monoclinic stacking faults on triclinic $K_2Cr_2O_7$ was the cause of its unusual external morphology. Polymorphism in dichromate-like compounds, however, has not been adequately studied to verify the existence of the complete sequence. The normal ambient form of $K_2Cr_2O_7$ is structure V[6,17–19] and is thought[11,20] to transform at 542 K into structure VII. An electron-diffraction study of a monoclinic ($P2_1/c$) form of $K_2Cr_2O_7$ has also been reported,[21] but doubt has been cast on the correctness of the structure.[16] $Rb_2Cr_2O_7$ exists in at least four forms, three of which have been determined by single-crystal *X*-ray methods.[15,22,23] The fourth form is obtained by quenching from high temperature. The normal form[23] [Figure 5 (*c*)] undergoes a transition at 591 K[11] but the structural nature of the high-temperature form is unknown. Polymorphism in $Cs_2Cr_2O_7$[24] and $(NH_4)_2Cr_2O_7$[25] has been established but the crystal structure of only one form of $(NH_4)_2Cr_2O_7$ is known,[26] whilst no structure for $Cs_2Cr_2O_7$ has been reported. Other dichromate-like compounds with these structures ($Cd_2P_2O_7$,[27] $Pb_2V_2O_7$,[28,29] and $K_2S_2O_7$[30]) are not known to undergo polymorphic transformations.

In structures I—X the pyroanions of a sheet pack so that the oxygen atoms of their 'backbones' adopt an approximately close-packed arrangement. Two dichromate-like structures which pack in a 'square-on' fashion are those of α-$Ca_2P_2O_7$[31] and α-$Sr_2P_2O_7$.[32,33] The G rare-earth disilicate structure* is isostructural with α-$Ca_2P_2O_7$ and is adopted by $Ln_2Si_2O_7$ (Ln = La, Ce, Pr, Nd,

* For an explanation of the symbolism A—G of the rare-earth disilicate structures, see refs. 34 and 35.

[20] U. Klement and G. M. Schwab, *Z. Krist.*, 1960, **114**, 170.
[21] L. A. Zhukova and Z. G. Pinsker, *Soviet Phys. Cryst.*, 1964, **9**, 31.
[22] P. Lofgren, *Acta Chem. Scand.*, 1971, **25**, 44.
[23] N. C. Panagiotopoulos and I. D. Brown, *Canad. J. Chem.*, 1970, **48**, 537
[24] R. L. Carter and C. E. Bricker, *Spectrochim. Acta*, 1973, **29A**, 253.
[25] I. H. Park, *Bull. Chem. Soc. Japan*, 1972, **45**, 2749.
[26] A. Bystrom and K. A. Wilhelmi, *Acta Chem. Scand.*, 1951, **5**, 1003; G. A. P. Dalgaard, A. C. Hazell, and R. G. Hazell, *Acta Chem. Scand.* (*A*), 1974, **28**, 541.
[27] C. Calvo and P. K. L. Au, *Canad. J. Chem.*, 1969, **47**, 3409.
[28] A. Kawahara, *Bull. Soc. Franc. Minérale Crist.*, 1967, **90**, 279.
[29] R. D Shannon and C. Calvo, *Canad. J Chem.*, 1973, **51**, 70.
[30] H. Lynton and M. R. Truter, *J. Chem. Soc.*, 1960, 5112.
[31] C. Calvo, *Inorg. Chem.*, 1968, **7**, 1345.
[32] J.-C. Grenier and R. Masse, *Bull. Soc. Franc Minérale Crist.*, 1967, **90**, 285.
[33] L.-O. Hagman, I. Jansson, and C. Magneli, *Acta Chem. Scand.*, 1968, **22**, 1419.

and Sm).[34-37] As in $Cd_2P_2O_7$(I)[27] and $Rb_2Cr_2O_7$(X),[15] the bridging oxygen atom in α-$Ca_2P_2O_7$ and α-$Sr_2P_2O_7$ does not participate in bonding with the cations, thus lacking a feature normally associated with dichromate-like structures. The F rare-earth disilicate structure[34,35] of $Eu_2Si_2O_7$ and $Sm_2Si_2O_7$ is thought to be very similar to the G structure since *X*-ray powder patterns are almost identical. The β-form of $Ca_2P_2O_7$[38] has structure III of the Brown and Calvo[16] scheme, in which the sheet stacking repeats in the crystal *z* direction after each fourth sheet; hence the *c*-axis (2414.4 pm) is approximately twice the length normally found in the stacking direction of dichromate-like structures (1266 pm in α-$Ca_2P_2O_7$). The A rare-earth disilicates $Sm_2Si_2O_7$[39] and $Pr_2Si_2O_7$[36] are isostructural with β-$Ca_2P_2O_7$, and *X*-ray powder patterns suggest that the low-temperature forms of $Nd_2Si_2O_7$ and $La_2Si_2O_7$ also have this structure.[34,35] Although the β-(A-) forms of these compounds may be considered as 'superstructures' of their α-(G-)forms, the considerable structural differences between the polymorphs, *e.g.* the packing of the 'backbones' of the pyroanions and the bonding of the bridging oxygen atom to cations, cause the $\beta \rightarrow \alpha$ (A→G) transition to be irreversible.[31] β-$Sr_2V_2O_7$[40] is isostructural with β-$Ca_2P_2O_7$ but the *X*-ray powder pattern of the high-temperature α-$Sr_2V_2O_7$ does not indicate it to be an isostructure of α-$Ca_2P_2O_7$ (XI) or of α-$Sr_2P_2O_7$ (XII).[41]

B. Other Dichromate-like Structures.—Numerous other dichromate-like structures which do not fit into any of the Brown and Calvo[16] categories are known. The largest group of such structures is that found in the melilite series of minerals. Mineral members of the melilite series which have had their structures determined by single-crystal methods include gehlenite, $Ca_2Al(SiAlO_7)$,[42] hardystonite, $Ca_2Zn(Si_2O_7)$,[43,44] and an intermediate melilite of composition $(Ca_{1.7}Na_{0.2}K_{0.1})(Mg_{0.5}Al_{0.4})(Si_{2.0}O_7)$.[45,46] Numerous synthetic melilites have been prepared and the structures of $(NaCa)Al(Si_2O_7)$, $(NaCa)Ga(Si_2O_7)$,[47] and $Y_2SiBe_2O_7$[48] have been determined. Amongst the natural melilites which have been examined by powder methods are akermanite, $Ca_2Mg(Si_2O_7)$[49] and gugiaite, $Ca_2Be(Si_2O_7)$.[50] In melilites the pyroanions pack 'perpendicularly'

[34] J. Felsche, *J. Less-Common Metals*, 1970, **21**, 1.
[35] J. Felsche, *Structure and Bonding*, 1973, **13**, 99.
[36] J. Felsche, *Z. Krist.*, 1971, **133**, 304.
[37] Yu. I. Smolin and Yu. F. Shepelev, *Acta Cryst.*, 1970, **B26**, 484.
[38] N. C. Webb, *Acta Cryst.*, 1966, **21**, 942.
[39] Yu. I. Smolin, Yu. F. Shepelev, and I. K. Butikova, *Kristallografiya*, 1970, **15**, 256.
[40] J. A. Baglio and J. N. Dann, *J. Solid State Chem.*, 1972, **4**, 87.
[41] A. A. Fotiev and V. A. Makarov, *Soviet Phys. Cryst.*, 1970, **14**, 621.
[42] F. Raaz, *Akad. Wiss., Wien*, 1930, **139**, 645.
[43] B. E. Warren and O. R. Trautz, *Z. Krist.*, 1930, **75**, 525.
[44] S. J. Louisnathan, *Z. Krist.*, 1969, **130**, 427.
[45] B. E. Warren, *Z. Krist.*, 1930, **74**, 131.
[46] J. V. Smith, *Amer. Mineralogist*, 1953, **38**, 643.
[47] H. Schichl and F. Raaz, *Akad. Wiss., Wien.*, 1968, 361; S. J. Louisnathan, *Z. Krist.*, 1970, **131**, 314.
[48] S. F. Bartram, *Acta Cryst.*, 1969, **B25**, 791.
[49] G. Ervin and E. F. Osborn, *Amer. Mineralogist*, 1949, **34**, 717.
[50] C. Peng, R. Tsao, and Z. Zou, *Scientia Sinica*, 1962, **11**, 977.

[Figure 6 (*a*)]. Similar packings of pyroanions are found in fresnoitite, $Ba_2(TiO)Si_2O_7$,[51] $SrCr_2O_7$,[52] and $Li_6Si_2O_7$.[53] Surprisingly, $Li_6Si_2O_7$ is the only simple alkali-metal or alkaline-earth-metal pyrosilicate whose crystal structure is known.

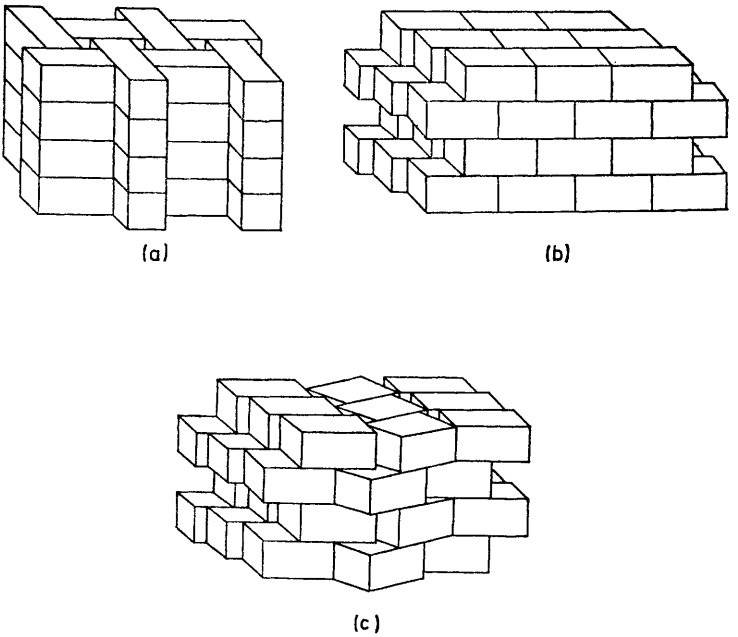

Figure 6 *Schematic representations of the packing geometry of pyroanions in pyro-structures: (a) 'perpendicular'; (b) 'end-on'; (c) 'skew'. Each* 2 × 1 × 1 *block represents a pyroanion in any possible conformation.*

Structures in which the packing of the pyroanions geometrically corresponds to the 'end on' arrangement of Figure 6 (*b*) include the α- and the β-forms of $Na_2Cr_2O_7$[54,55] and synthetic 'y-phase' yttrialite, $Y_2Si_2O_7$.[56] However, in y-$Y_2Si_2O_7$ the pyroanions are in an exactly eclipsed conformation, but are substantially skew in both forms of $Na_2Cr_2O_7$. β-$Na_2Cr_2O_7$, the ambient-temperature form,[55] contains two crystallographically distinct dichromate anions, one being truly dichromate-like and the other more thortveitite-like, having an almost staggered conformation. The β→α transition occurs at 513 K and, unlike

[51] P. B. Moore and J. Louisnathan, *Nature*, 1967, **215**, 1361.
[52] K. A. Wilhelmi, *Arkiv Kemi*, 1966, **26**, 149.
[53] H. Vollenke, A. Wittman, and H. Nowotny, *Monatsh.*, 1969, **100**, 295.
[54] N. C. Panagiotopoulos and I. D. Brown, *Acta Cryst.*, 1973, **B29**, 890.
[55] N. C. Panagiotopoulos and I. D. Brown, *Acta Cryst.*, 1972, **B28**, 1352.
[56] N. G. Batalieva and Yu. A. Pyatenko, *Kristallografiya*, 1971, **16**, 905

the V→VII transition of $K_2Cr_2O_7$, does not destroy the crystal. In the α-$Na_2Cr_2O_7$ structure[54] all the dichromate ions have an intermediate conformation. The β→α phase transition therefore involves small movements of atoms which result in crystallographically different pyroanions of the β-form becoming identical in the α-form. $Ag_2Cr_2O_7$ is thought to be isostructural with α-$Na_2Cr_2O_7$, but only a preliminary report of its structure has been given.[57]

Other structures with 'end-on' packings of pyroanions are those of the ambient-temperature forms of $Na_4As_2O_7$,[58] $Na_4P_2O_7$,[59] $Na_3ScSi_2O_7$,[60] and $Na_2Zn_2Si_2O_7$.[61] $Na_4As_2O_7$ undergoes a series of slowly reversible transitions between ambient temperature and 500 K and a further reversible transition at 953 K, but structural data for the high-temperature polymorphs are not available. The ambient-temperature form of $Na_4P_2O_7$,[59] which is not isostructural with $Na_4As_2O_7$, also undergoes several phase transitions[62,63] which have been related to disorder in the bridging oxygen atom that is bonded to only one cation and has a large vibration amplitude. Other $M_4X_2O_7$ compounds which show numerous phase transitions include $Li_4As_2O_7$ and $Li_4P_2O_7$.[64]

Intermediate between the 'perpendicular' packings of melilite-type structures and the various 'end-on' structures are a group of structures in which the pyroanions adopt a 'skew' packing [Figure 6 (*c*)]. All of the sheet structures incorporated in the Brown and Calvo[16] scheme, with the exception of structures I and X of Table 1 are of this type. Other structures of this type are those of $NaRbCr_2O_7$ [65] $Er_2Ge_2O_7$,[66] and the E rare-earth disilicate structure (adopted by the disilicates of Y, Ho, Dy, Eu, and Gd[35,37]). $Er_2Ge_2O_7$ is the only pyrogermanate which has been studied by single-crystal methods (the pyrogermanates of Tb, Dy, Ho, Yb, and Y have been shown to be isostructural by powder methods[66]). In Figure 1 the structural transition from dichromate-like structures to thortveitite-like structures is shown to occur for the pyrosilicates and pyrogermanates as the radius of the cation, $r(^{cn}M^{m+})$, decreases below about 90 pm and 100 pm, respectively. Felsche[34,35] has shown that the largest rare-earth cation which adopts a thortveitite-like structure in the pyrosilicate series is $Ho^{3+}[r(^{VI}Ho^{3+}) = 89$ pm] although $Eu^{3+}[r(^{VI}Eu^{3+}) = 95$ pm] is the smallest cation which adopts a truly dichromate-like structure. The ambient-temperature form of the disilicates of cations of radii between 89 and 95 pm adopts the B rare-earth structure, which contains both $Si_3O_{10}^{8-}$ and SiO_4^{4-} anions. On this basis, the pyrogermanate of $Er^{3+}[r(^{VI}Er^{3+}) = 88$ pm] would be expected to have

[57] R. G. Hazell, *Acta Cryst.*, 1969, **A25**, S116.
[58] K. Y. Leung and C. Calvo, *Canad. J. Chem.*, 1973, **51**, 2082.
[59] K. Y. Leung and C. Calvo, *Canad. J. Chem.*, 1972, **50**, 2519.
[60] S. M. Skshat, V. I. Simonov, and N. V. Belov, *Doklady Akad. Nauk S.S.S.R.*, 1969, **184**, 337.
[61] S. T. Amirov, A. V. Nikitin, V. V. Ilyukhin, and N. V. Belov, *Doklady Akad. Nauk S.S.S.R.*, 1967, **177**, 92.
[62] K. Y. Leung, *Canad. J. Chem.*, 1975, **53**, 1739.
[63] E. M. Kurian and R. V. Tamhankar, *Proc. Chem. Symp. Madras*, 1970, **2**, 143.
[64] F. Remy, *Bull. Soc. chim. France*, 1969, 3380.
[65] N. C. Panagiotopoulos and I. D. Brown, *Acta Cryst.*, 1972, **B28**, 2880.
[66] Yu. I. Smolin, *Soviet Phys. Cryst.*, 1970, **15**, 36.

a thortveitite-like structure, and although it possesses some thortveitite-like features it is here classified as dichromate-like, since the Ge—O′—Ge angle is 136° and the three smallest torsion angles (2°, 36°, and 36°) indicate the anion to be essentially eclipsed. However, the conformation of the anion [Figure 7]

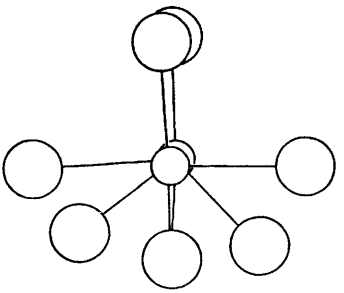

Figure 7 *Conformation of the* $Ge_2O_7^{6-}$ *anion of* $Er_2Ge_2O_7$.

is unusual in being almost ideally eclipsed on one side and almost ideally staggered on the other. Also, O′ does not enter into the primary co-ordination of the Er^{3+} ion. The $Er_2Ge_2O_7$ structure therefore shows features of both major structural types, and indicates that further structural studies of rare-earth pyro-compounds (for example dichromates and diarsenates) are required before the influence of ionic radii on the structures and stability fields[67] of these compounds is fully understood.

3 Thortveitite-like Structures

A. Thortveitite and its Hettotypes.*—The principal features of thortveitite-like structures are (i) a staggered conformation of the pyroanion, (ii) a bridging angle in excess of 140°, (iii) no co-ordination between any cation and the bridging oxygen atom. Thortveitite is a rare mineral of approximate composition $Sc_2Si_2O_7$ but with considerable isomorphous replacement of Sc, principally by Y and Fe. The structure of this mineral has been the subject of some controversy since Zachariasen[68] first reported it to crystallize in space group $C2/m$, with a linear Si—O′—Si bridge. Subsequent pyrosilicate structures were found to contain bent Si—O′—Si bridges, and the linear bridge of $Sc_2Si_2O_7$ was disputed.[69] A thorough reinvestigation[5] of the thortveitite structure, however, confirmed Zachariasen's results, and linear Si—O′—Si bridges have now been unambiguously established

* For a set of related structures the simplest and most symmetrical structure is termed the aristotype. Less symmetrical variants of the aristotype are termed hettotypes. The repeat unit of a hettotype may contain several of the original repeat units of the aristotype and is said to be uni-, bi-, tri-partite *etc.* according to the number of aristotype units it contains. (See ref. 82.)

[67] R. D. Shannon and C. T. Prewitt, *J. Solid State Chem.*, 1970, **2**, 199.
[68] W. H. Zachariasen, *Z. Krist.*, 1930, **73**, 1.
[69] F. Liebau, *Acta Cryst.*, 1961, **14**, 1103.

in numerous structures (*e.g.* $Yb_2Si_2O_7$[70] and $Er_2Si_2O_7$[37]). A projection of the $Si_2O_7^{6-}$ packing in the thortveitite (or C rare-earth disilicate) structure is shown in Figure 8. The cations are approximately octahedrally co-ordinated by the

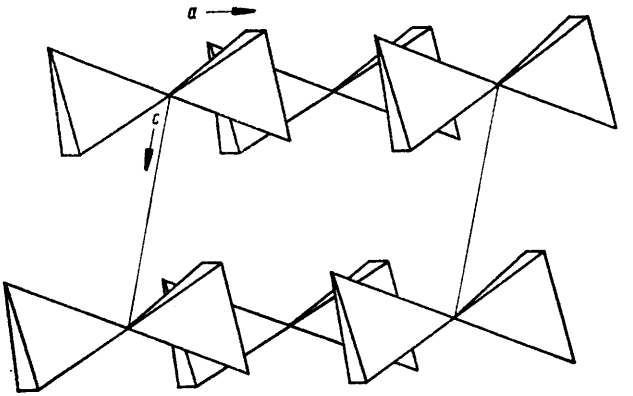

Figure 8 *Projection of the thortveitite* ($Sc_2Si_2O_7$) *structure, showing the packing of the* $Si_2O_7^{6-}$ *anions.*

terminal oxygen atoms of the pyroanions, resulting in a structure which approximates to a hexagonally close-packed arrangement of terminal oxygen atoms.[71] The bridging oxygen atoms lie between the close-packed layers and cause the *a*-axis to be about 25% longer than predicted from an ideally close-packed model.[72,73]

In contrast to the dichromate-like structures in which isotypism is rare, the stability field of the thortveitite structure is wide, and a great many substances have been reported to adopt this structure.[74–81] Most of these have been studied only by powder methods, but single-crystal determinations of ten isotypes have been reported (Table 2). In all of these compounds the *X*-ray thermal parameters indicate high disorder at the bridging oxygen atom. This is normally interpreted as the result of high thermal vibration, particularly in the plane perpendicular to the X–X axis, rather than of positional disorder.

Four compounds listed in Table 2, β-$Mg_2P_2O_7$, β-$Ni_2P_2O_7$, β-$Cu_2P_2O_7$, and

[70] Yu. I. Smolin, Yu. F. Shepelev, and I. K. Butikova, *Zhur. strukt. Khim.*, 1971, **12**, 272.
[71] G. M. Clark, 'The Structures of Non-molecular Solids', Applied Science, London, 1972, p. 323.
[72] P. K. L. Au and C. Calvo, *Canad. J. Chem.*, 1967, **45**, 2297.
[73] C. Calvo and K. Neelakantan, *Canad. J. Chem.*, 1970, **48**, 890.
[74] K. Lukaszewicz, *Bull. Acad. polon. Sci., Sér. Sci. chim.*, 1963, **11**, 361.
[75] K. Lukaszewicz, *Roczniki Chem.*, 1961, **35**, 31.
[76] C. Calvo, *Canad. J. Chem.*, 1965, **43**, 1139.
[77] K. Lukaszewicz and R. Smajkiewicz, *Roczniki Chem.*, 1961, **35**, 741.
[78] A. Pietraszko and K. Lukaszewicz, *Bull. Acad. polon. Sci., Sér .Sci. chim.*, 1968, **16**, 183.
[79] B. E. Robertson and C. Calvo, *Canad. J. Chem.*, 1968, **46**, 605.
[80] C. Calvo, *Canad. J. Chem.*, 1965, **43**, 1147.
[81] E. Dorm and B.-O. Marinder, *Acta Chem. Scand.*, 1967, **21**, 590.

Table 2 *Single-crystal determinations of thortveitite isotypes*

Compound	*Reference*
$Sc_2Si_2O_7$	*a*
$Mg_2As_2O_7$	*b*
β-$Mg_2P_2O_7$	*c*
$Mn_2P_2O_7$	*d*
β-$Ni_2P_2O_7$	*e*
β-$Cu_2P_2O_7$	*f*
β-$Zn_2P_2O_7$	*g*
$Yb_2Si_2O_7$	*h*
$Mn_2V_2O_7$	*i*
$Cd_2V_2O_7$	*j*

[a] D. W. J. Cruickshank, H. Lynton, and G. A. Barclay, *Acta Cryst.*, 1962, **15**, 491; [b] C. Calvo and K. Neelakantan, *Canad. J. Chem.*, 1970, **48**, 890; [c] C. Calvo, *Canad. J. Chem.*, 1965, **43**, 1139; [d] K. Lukaszewicz and R. Smajkiewicz, *Roczniki Chem.*, 1961, **35**, 741; [e] A. Pietraszko and K. Lukaszewicz, *Bull. Acad. polon. Sci., Ser. Sci. chim.*, 1968, **16**, 183; [f] B. E. Robertson and C. Calvo, *Canad. J. Chem.*, 1968, **46**, 605; [g] C. Calvo, *Canad. J. Chem.*, 1965, **43**, 1147; [h] Yu. I. Smolin and Yu. F. Shepelev, *Acta Cryst.*, 1970, **B26**, 484; [i] E. Dorm and B.-O. Marinder, *Acta Chem. Scand.*, 1967, **21**, 590; [j] P. K. L. Au and C. Calvo, *Canad. J. Chem.*, 1967, **45**, 2297.

β-$Zn_2P_2O_7$, are high-temperature polymorphs. The low-temperature (α-)forms have structures which are multipartite hettotypes[82] of thortveitite. Three varieties have been found:

(i) the α-$Cu_2P_2O_7$ structure,[83,84] in which the *c*-axis of the β-(thortveitite) form is doubled;

(ii) the α-$Mg_2P_2O_7$[85,86] and α-$Ni_2P_2O_7$[87] structure, in which both the *a*- and the *c*-axes are doubled;

(iii) the α-$Zn_2P_2O_7$ structure,[88] in which the *a*-axis is tripled and the *c*-axis is doubled.

α-$Zn_2V_2O_7$[89] and β-$Cu_2V_2O_7$[90] (and probably $NaAlP_2O_7$ and $NaFeP_2O_7$-II[91,92]) are isostructural with α-$Cu_2P_2O_7$. α-$Co_2P_2O_7$[93] is isostructural with α-$Mg_2P_2O_7$ and α-$Ni_2P_2O_7$. Apart from the increases in cell dimensions, the structurally significant difference between the hettotypes and the arisototype (thortveitite itself) is the magnitude of the X—O′—X angle, which ranges from 137° in

[82] I. Lefkowitz, K. Lukaszewicz, and H. D. Megaw, *Acta Cryst.*, 1966, **20**, 670.
[83] K. Lukaszewicz, *Bull. Acad. polon. Sci , Sér. Sci. chim.*, 1966, **14**, 725.
[84] B. E. Robertson and C. Calvo, *Acta Cryst.*, 1967, **22**, 665.
[85] K. Lukaszewicz, *Bull. Acad. polon. Sci., Sér. Sci. chim.*, 1967, **15**, 53.
[86] C. Calvo, *Acta Cryst.*, 1967, **23**, 289.
[87] K. Lukaszewicz, *Bull. Acad. polon. Sci., Sér Sci. chim.*, 1967, **15**, 47.
[88] B. E. Robertson and C. Calvo, *J. Solid State Chem.*, 1970, **1**, 120.
[89] R. Gopal and C. Calvo, *Canad. J. Chem.*, 1973, **51**, 1004.
[90] D. Mercurio-Lavaud and B. Frit, *Compt. rend.*, 1973, **277**, 1101.
[91] J.-P. Gamondès, F. D'Yvoire, and A. Boullé, *Compt. rend.*, 1971, **272**, 49.
[92] H. N. Ng and C. Calvo, *Canad. J. Chem.*, 1973, **51**, 2613
[93] N. Krishnamachari and C. Calvo, *Acta Cryst.*, 1972, **B28**, 2883.

α-$Ni_2P_2O_7$ to 157° in α-$Cu_2P_2O_7$. In no case, however, does the bridging oxygen atom co-ordinate with any cation; thus the primary features of the thortveitite-like character are retained in the α-forms.

The α–β phase transformations of the pyrophosphates, particularly of Mg, Ni, Cu, and Zn, have been studied in some detail, using a variety of thermoanalytical, spectrochemical, and high-temperature *X*-ray techniques.[83–100] Transformation mechanisms appear to be complex, and occur slowly and diffusely over temperature ranges of up to 20 degrees.

The polymorphs and polymorphic transformations of the pyrovanadates are less well studied. α-$Zn_2V_2O_7$ is a hettotype of thortveitite that is isotypic with α-$Cu_2P_2O_7$, and the powder pattern of β-$Zn_2V_2O_7$ indicates it to be isotypic with thortveitite.[89,101] An orthorhombic phase of $Zn_2V_2O_7$ has also been reported,[102] the cell dimensions of which indicate that it may be isotypic with α-$Cu_2V_2O_7$.[103,104]

β-$Cu_2V_2O_7$,[90] the stable form of $Cu_2V_2O_7$ above 985 K,[105] is isotypic with α-$Zn_2V_2O_7$ and α-$Cu_2P_2O_7$. The low-temperature α-form[103,104] is not a thortveitite hettotype but contains a staggered $V_2O_7^{4-}$ ion, showing the structure to be thortveitite-like. Comparison of the α- and β-forms of $Cu_2V_2O_7$ indicates that the α–β transition is mechanistically complex, involving the breakage of at least three Cu—O bonds and inversion and rotation of $V_2O_7^{4-}$ anions. Such a mechanism appears somewhat complex for a reversible transformation, although in the β→α direction it proceeds with difficulty, particularly after fusion. A further (monoclinic) form of $Cu_2V_2O_7$ has been reported[106] to form in solid–solid preparations below the melting point. The cell dimensions indicate that this form may be isotypic with thortveitite.

Phase transformations in $Mg_2V_2O_7$ are also complex. One form (β-),[107] obtained from the cooling of a melt, has a structure related to that of thortveitite but in which there is a fifth weak bond between each vanadium atom and a terminal oxygen atom of a neighbouring $V_2O_7^{4-}$ anion. This represents a new type of structure, unknown in the corresponding pyrophosphates, presumably arising from the ability of V^{5+} to adopt four-, five-, and six-fold co-ordination with almost equal ease.[108] The α-form of $Mg_2V_2O_7$ is obtained on annealing β-$Mg_2V_2O_7$ below 970 K,[12,13] and its *X*-ray powder pattern indicates it to be

[94] R. Roy, E. T. Middleswarth, and F. A. Hummel, *Amer. Mineralogist*, 1948, **33**, 458
[95] F. L. Oetting and R. A. McDonald, *J. Phys. Chem.*, 1963, **67**, 2757.
[96] A. N. Lazarev and T. F. Tenisheva, *Izvest. Akad. Nauk S.S.S.R.*, 1964, 242.
[97] C. Calvo, W. R. Datars, and J. S. Leung, *J. Chem. Phys.*, 1967, **46**, 796.
[98] J. Sarver, *Trans. Brit. Ceram. Soc.*, 1966, **65**, 191.
[99] F. L. Katnack and F. A. Hummel, *J. Electrochem. Soc.*, 1955, **105**, 125.
[100] J. G. Chambers, W. R. Datars, and C. Calvo, *J. Chem. Phys.*, 1964, **41**, 806.
[101] G. M. Clark and A. N. Pick, *J. Thermal Analysis*, 1975, **7**, 289.
[102] J. Angenault, *Rev. Chim. minérale*, 1970, **7**, 651.
[103] D. Mercurio-Lavaud and B. Frit, *Acta Cryst.*, 1973, **B29**, 2737.
[104] C. Calvo and R. Faggiani, *Acta Cryst.*, 1975, **B31**, 603.
[105] P. Fleury, *Rev. Chim. minérale*, 1969, 6, 819.
[106] J. C. Pedregosa, E. J. Baran, and P. G. Aymonino, *Z. Krist.*, 1973, **139**, 221.
[107] R. Gopal and C. Calvo, *Acta Cryst.*, 1974, **B30**, 2491.
[108] H. G. Bachmann and W. H. Barnes, *Z. Krist.*, 1961, **115**, 215.

fully isomorphous with the pyrovanadates of cobalt and nickel.[14] The α–β transformation of $Mg_2V_2O_7$, like those of $Cu_2V_2O_7$ and $Mg_2P_2O_7$, is reversible only with difficulty, and the two forms co-exist at 990 K.[12] A second rapidly reversible phase transition occurs at 1183 K but the structure of the high-temperature (γ-)form is not known. The monoclinic phase of $Mg_2V_2O_7$ reported by Pedregosa *et al.*[106] and suggested to be isotypic with α-$Mg_2P_2O_7$ is probably the form designated α-$Mg_2V_2O_7$, isotypic with $Co_2V_2O_7$.

Although, from the point of view of ratios of ionic radii (Figure 1), $Co_2V_2O_7$ and $Ni_2V_2O_7$[14] would be expected to exhibit thortveitite-like structures, they show several features related to dichromate-like structures. Thus the bridging angles are 117—118°, the conformations of the pyroanions are essentially eclipsed, and the bridging oxygen atoms partake in the octahedral co-ordination of the cations. Further, the anions are packed in a similar columnar manner to the anions in the dichromate-like α-$Sr_2P_2O_7$.[32,33] However, the edge-sharing between cation octahedra in $Co_2V_2O_7$ is similar to that in thortveitite, and serves to illustrate that distinctions of structural type based solely on anion configuration may be misleading, especially when applied to border regions of the stability field.

The assumption that the $Co_2V_2O_7$ structure is dichromate-like makes $Mg_2V_2O_7$ unique in being the only known compound containing a pyroanion which can transform between a dichromate-like form (α-$Mg_2V_2O_7$) and a thortveitite-like form (β-$Mg_2V_2O_7$)*.

It is apparent from Figure 1 that only compounds $M_2X_2O_7$ with the smaller $r(M)/r(X)$ ratios exhibit polymorphism. For example, of the pyro-compounds listed in Table 2, only the pyrophosphates and pyrovanadates of the smaller cations (Mg^{2+}, Co^{2+}, Ni^{2+}, Cu^{2+} and Zn^{2+}) show low-temperature α-forms. $Mn_2V_2O_7$, $Cd_2V_2O_7$, $Mn_2P_2O_7$, *etc.*, which have larger $r(M)/r(X)$ ratios, have not been found to exhibit polymorphism.[88,101] Further studies, for example of transition-metal pyrogermanates, pyroarsenates,[109] and dichromates and their phase transitions, will be required before the complex inter-relationships between thortveitite and its hettotypes are fully understood.

B. Other Thortveitite-like Structures.—Although it is the highest-temperature polymorph of the above compounds that generally adopts the thortveitite structure, in $Er_2Si_2O_7$ a further transformation[34,35] occurs at around 1670 K to the D rare-earth pyrosilicate structure.[37] This structure, which is also known for $Y_2Si_2O_7$,[110] is similar to the thortveitite structure in having linear staggered $Si_2O_7^{6-}$ anions containing highly vibrant bridging oxygen atoms which do not enter into the octahedral co-ordination of the rare-earth cation. However, the anion packing in thortveitite is of the 'end-on' type, whereas that of D-$Er_2Si_2O_7$ is 'skew' [Figure 6]. The D rare-earth disilicate structure is of special interest

* Powder data suggest that $Ho_2Si_2O_7$ may transform at 1850 K from the thortveitite-like D rare-earth disilicate structure to the dichromate-like E rare-earth disilicate structure.[55] $Y_2Si_2O_7$ may also transform between the two major types.[56,110]

[109] J. Ozog, N. Krishnamachari, and C. Calvo, *Canad. J. Chem.*, 1970, **48**, 388.

[110] N. G. Batalieva and Yu. A. Payatenko, *Zhur. strukt. Khim.*, 1968, **11**, 921.

because it provides direct evidence for linear Si—O′—Si bonds. The space group is $P2_1/b$, and since $Z = 2$ the $Si_2O_7^{6-}$ ions must necessarily occupy the two-fold special positions; hence the linearity of the Si—O′—Si linkage is established without recourse to structure refinements, as are necessary in the case of thortveitite.[5]

Linear pyroanions have also been established in ZrP_2O_7,[111,112] but a more recent refinement[113] indicates that this structure contains linear pyroanions only as a result of positional disorder of the bridging oxygen atom and that the true P—O′—P angle is about 150°. Above 570 K superstructure lines indicating a supercell of cell dimension three times that of the low-temperature form are found in *X*-ray photographs.[114,115] However, this transformation does not appear to be reversible, a third form, having a slightly different cell dimension to that of the previous low-temperature form, being produced.[113] A number of isotypes of ZrP_2O_7 have been reported, including the pyrophosphates of Si, Ge, Ti, Zr, Sn, Th, and U. SiP_2O_7 is known in several modifications, designated AI (ZrP_2O_7 type), AIII, and AIV.[116,117] The AIII form is unusual in containing octahedrally co-ordinated Si atoms, but, in spite of a small P—O′—P angle (139°), the bridging oxygen atom does not enter into the Si co-ordination.

The smallest P—O′—P angle reported to date is 123°, found in $KAlP_2O_7$.[92] However, the anion is nearly ideally staggered, and the bridging oxygen atom co-ordinates only weakly to the K^+ cation and not to the Al^{3+} cation. It has been suggested,[91] on the basis of powder photographs, that $KAlP_2O_7$ is isostructural with $NaFeP_2O_7$-I, which transforms irreversibly into $NaFeP_2O_7$-II, with the α-$Cu_2P_2O_7$ structure. $KAlP_2O_7$ has not been found to transform.

The barysilite structure[118,119] offers a further example of a structure possessing a conformationally staggered pyroanion with a small bridging angle. The composition of barysilite is given by the formula $XY_2Pb_6(Z_2O_7)_3$, where Z = Si or Ge, Y = Pb, X = various bivalent cations, *e.g.* Mg, Ca, Ba, Mn, Fe, Co, Ni, Zn, or Pb. Two barysilites have been studied as single crystals; $MnPb_8(Si_2O_7)_3$[120] and $Pb_3Si_2O_7$ [*i.e.* $(Pb\ Pb_2)Pb_6(Si_2O_7)_3$].[121] In this complex structure, $Si_2O_7^{6-}$ ions are linked by trigonally co-ordinated Pb^{2+} ions into a framework containing channels parallel to the *c*-axis of the hexagonal cell. Within these channels are located chains of the remaining cations; hence the formula, from a structural standpoint, is XY_2 $[Pb_6(Si_2O_7)_3]$, where X is any cation capable of entry into the channels. In $Pb_3Si_2O_7$ the Si—O′—Si angle is 125° and represents the smallest

[111] G. R. Levi and G. Peyronel, *Z. Krist.*, 1935, **92**, 190.
[112] H. M. McGeachin, *Acta Cryst.*, 1961, **14**, 1286.
[113] M. Chaunac, *Bull. Soc. chim. France*, 1971, 424.
[114] C.-H. Huang, O. Knop, D. A. Othen, F. W. D. Woodhams, and R. A. Howie, *Canad. J. Chem.*, 1975, **53**, 79.
[115] L.-O. Hagman and P. Kierkegaard, *Acta Chem. Scand.*, 1969, **23**, 327.
[116] G. Bissert and F. Liebau, *Acta Cryst.*, 1970, **B26**, 233; E. Tillmanns, W. Gebert, and W. H. Baur, *J. Solid State Chem.*, 1973, **7**, 69.
[117] F. Liebau and K.-F. Hesse, *Naturwiss.*, 1969, **56**, 634; *Z. Krist.*, 1971, **133**, 213.
[118] H. W. Billhardt, *Amer. Mineralogist*, 1969, **54**, 510.
[119] A. B. Harnik, *Amer. Mineralogist*, 1972, **57**, 277.
[120] J. Lajzérowicz, *Acta Cryst.*, 1965, **20**, 357.
[121] W. Petter, A. B. Harnik, and U. Keppler, *Z. Krist.*, 1971, **133**, 445.

bridging angle reported for a pyrosilicate. The structures of $Na_2Zr(Si_2O_7)$,[122] $K_2Zr(Si_2O_7)$,[123] and $Na_2Mn_2(Si_2O_7)$[124] also feature essentially staggered anions, with bridging angles less than 150°. A further feature is that the bridging oxygen atom co-ordinates only with the M^I cation.

A considerable number of complex mineral pyrosilicates in which $Si_2O_7^{6-}$ anions, often in association with SiO_4^{4-} and OH^- ions, are counterbalanced by a variety of isomorphously replaced cations have been studied. Examples include fresnoite,[51] hemimorphite,[125] epidote,[126] allanite,[126] hancockite,[126] barylite,[127] picmonite,[128] zoisite,[129] clinozoisite,[129] tillyite,[130] and lead glass,[131] but these are not considered here.

4 Bonding in Pyro-compounds

A. Bond Lengths.—The nature of the chemical bonding and the relationship between bond lengths and bond strengths in $X_2O_7^{n-}$ pyroanions have been the subject of much discussion. Historically, the first step was made by Pauling,[132] with the exposition of the electrostatic valence principle, which stated that in a stable system the sum of the strengths of the electrostatic valence bonds which reach any anion, X, from all its neighbouring cations, A, is equal to the charge, z_X, of that anion. The strength of the electrostatic valence bond (S_i) is given by z_A/n_A, where z_A is the formal charge of the cation A and n_A is its co-ordination number. The principle can therefore be expressed as

$$p_X = \sum_{i=1}^{n} S_i = z_X$$

In isolated pyroanions the bridging oxygen atom (O′) obeys this principle only in $Si_2O_7^{6-}$, since the sum, p_X, of the strengths of the bonds reaching O′ is $\frac{4}{4} + \frac{4}{4} = 2$. Considerable deviations occur in $X_2O_7^{n-}$, where X = Cr, V, P, S *etc.*, a fact often quoted in explanation of the non-occurrence of these ions in natural minerals. However, truly isolated pyroanions do not occur in any pyro-compound; for example terminal oxygen atoms always bond to one or more cations, and in dichromate-like structures the bridging oxygen atom commonly

[122] A. A. Voronkov, N. G. Shumyatskaya, and Yu. A. Pyatenko, *Zhur. strukt. Khim.*, 1970, **11**, 932.
[123] A. N. Chernov, B. A. Maksimov. V. V. Ilyukhin, and N. V. Belov, *Doklady Akad. Nauk S.S.S.R.*, 1970, **193**, 1293.
[124] L. P. Astakhova, E. A. Pobedimskaya, and V. I. Simonov, *Doklady Akad. Nauk S.S.S.R.*, 1967, **173**, 1401.
[125] W. S. McDonald and D. W. J. Cruickshank, *Z. Krist.*, 1967, **124**, 180.
[126] W. A. Dollase, *Amer. Mineralogist*, 1971, **56**, 447.
[127] E. Cannilo, A. Dal Negro, and G. Rossi, *Rend. Soc Ital. Min. Pet.*, 1969, **26**, 3.
[128] W. A. Dollase, *Amer. Mineralogist*, 1969, **54**, 710.
[129] W. A. Dollase, *Amer. Mineralogist*, 1968, **53**, 1882.
[130] J. V. Smith, *Acta Cryst.*, 1953, **6**, 9.
[131] T. Naray-Szabo, *Phys. and Chem. Glasses*, 1963, **4**, 38A.
[132] L. Pauling, *J. Amer. Chem. Soc.*, 1929, **51**, 1010.

co-ordinates to other cations. The contributions which all nearest neighbours make to p_x must therefore be accounted.

A priori, the proportion of its formal charge that a given anion distributes to its various neighbours will be related to the numbers, charges, and distances of these neighbours. The electrostatic valence principle accounts only for the numbers and charges. Pauling[133] first took account of the criterion of distance (bond length) in his theories of the metallic bond, for which he found that bond length and bond order could be related by the expression

$$r_{(1)} - r_{(n)} = 0.300 \log n$$

where $r_{(1)}$ is the bond length of a bond of order 1
$r_{(n)}$ is the bond length of a bond of order n
n is the bond number (the number of shared electron-pairs per bond).
Bystrom and Wilhelmi[26] first used an expression of this form in the context of pyro-compounds when they applied the relationship

$$r_{(1)} - r_{(n)} = 2\,k \log n$$

to $(NH_4)_2Cr_2O_7$. The arbitrary constant k was shown to be 0.39 and $r_{(1)}$ was 167 pm. Evans[134] subsequently found that for V^{5+}—O bonds $k = 0.39$ and $r_{(1)} = 181$ pm. Shannon and Calvo,[29] however, now find that the best overall value of $r_{(1)}$ for a single V^{5+}—O bond is 172.1 ± 1.2 pm.

The most systematic and comprehensive relationships between bond length, bond strength, and bond order in metal–oxygen systems have been given by Baur[135,136] and by Brown and Shannon.[137] Baur[135] noted that the p_x received by an individual anion varied directly with the bond lengths, d(A—X), formed by the anion. This relationship could be expressed for P^{5+}—O and Si^{4+}—O bonds, respectively, as

$$d(\text{Si—O}) = 1.44 + 0.09\,p_0$$
$$d(\text{P—O}) = 1.32 + 0.11\,p_0$$

Such relationships are useful in predicting bond lengths. Further, Baur[136] noted that the mean observed d(A—X) in a co-ordination polyhedron, $\langle d(\text{A—X})\rangle$, was related to d(A—X) and Δp_x, the difference between the p_x values of one individual anion in the co-ordination polyhedron around a cation and the mean p_x of all anions in the co-ordination polyhedron. This relationship took the general form

$$d(\text{A—X}) = \langle d(\text{A—X})\rangle + b\Delta p_x$$

and derived values of $\langle d(\text{A—X})\rangle$ and b for P^{5+}—O and Si^{4+}—O gave

$$d(\text{P—O}) = 1.537 + 0.109\,\Delta p_0$$
$$d(\text{Si—O}) = 1.622 + 0.091\,\Delta p_0$$

[133] L. Pauling, *J. Amer. Chem. Soc.*, 1947, **69**, 542.
[134] H. T. Evans, *Z. Krist.*, 1960, **114**, 257.
[135] W. H. Baur, *Trans. Amer. Cryst. Ass.*, 1970, **6**, 129.
[136] W. H. Baur, *Amer. Mineralogist*, 1971, **56**, 1573.
[137] I. D. Brown and R. D. Shannon, *Acta Cryst.*, 1973, **A29**, 266.

For the pyrosilicate anions of 26 pyrosilicate structures the absolute mean deviation of d(Si—O) calculated from the above expression and the observed d(Si—O) was found to be 1.0 pm.

Baur's extension of the electrostatic valence principle has been widely used for the prediction of bond lengths in pyro-compounds and in rationalizing the observed distortions of the component XO_4 tetrahedra. For example, the observed P—O bond lengths in $KAlP_2O_7$ have been compared [92] with the bond lengths calculated from Baur's d(P—O) expression. With the exception of the bond to O_4, which forms the shortest P—O (and Al—O) bond, the value of $|d_{obs} - d_{calc}|$ never exceeds 1.5 pm.

Corresponding extended electrostatic valence principle expressions for other X—O bonds have now been derived. For example, for V^{5+}—O bonds Calvo[29,89] has shown the following relationship to hold

$$d(\text{V—O}) = 1.721 + 0.160\,\Delta p_0$$

In the Baur[136] extension of the electrostatic valence principle it is assumed that a linear relationship exists between bond strength and bond length. Felshe[35] has incorporated an inverse-square relationship between charge and bond length by introducing the term $(\langle d\rangle/d_i)^2$ into the calculation of the individual electrostatic bond strengths s_i. Here d_i is the individual bond length d(A—X) and $\langle d\rangle$ is the mean bond length $\langle d(\text{A—X})\rangle$, and the general expression becomes

$$p_X = \sum_{i=1}^{n} (z_A/n_A)\,(\langle d\rangle/d_i)^2$$

This expression provides a remarkably good straight-line correlation between $[d(\text{Si—O}) - \langle d(\text{Si—O})\rangle]$ and Δp_0 for the rare-earth disilicates. However, the Felsche modification, by its use of observed bond lengths, loses the truly predictive capabilities of the Baur theory.

The non-linear relationship between bond strength and bond length has been expressed in various forms.[138–140] Recently, Brown and Shannon[137] have shown that the relationship due to Donnay and Allman[140] combines simplicity with reliability, and have adapted it for use in a wide range of simple and complex oxides. Their expression takes the form

$$S = S_0\,(R/R_0)^{-N}$$

where S is the individual bond strength, R is the individual bond length, S_0 is the bond strength associated with a bond of length R_0, and N is an arbitrary constant. Values of S_0, R_0, and N associated with a given cation were derived from a large number of crystal structures containing that cation by setting the sums of the individual bond strengths, S, around the cation as nearly as possible equal to its formal valence. On average, the sum of the bond strengths around an ion was shown to be within about 5% of its valence, even in cases where the

[138] W. H. Zachariasen, *Acta Cryst.*, 1963, **16**, 385.
[139] J. R. Clark, D. Appleman, and J. Papike, *Miner. Soc. Amer., Special Paper.* 1969, **2**, 31.
[140] G. Donnay and R. Allman, *Amer. Mineralogist*, 1970, **55**, 1003.

co-ordination around an ion was very distorted. This facility proves to be an advantage over the Baur[135,136] theory, which, as a consequence of its use of a linear bond length–bond strength relationship, is less satisfactory for highly distorted co-ordinations, *e.g.* as often found around V^{5+}.

In Tables 3—6, calculated bond-strength sums p_{Cr}, p_P, p_{Si}, and p_V (around the Cr^{6+}, P^{5+}, Si^{4+}, and V^{5+} cations) and the calculated bond-strength sum $p_{O'}$ (around the bridging oxygen atom) are collected with other pertinent crystal data for pyro-compounds. The mean values for p_{Cr}, p_P, p_V, and p_{Si} are 6.05, 5.03, 4.98, and 3.96, respectively, confirming that in general $p_X = z_X$, although for individual structures, even for some accurately determined structures, the deviation is large (see for example $P2_1/n$ $Rb_2Cr_2O_7$, $Co_2V_2O_7$, and β-$Cu_2P_2O_7$).

Table 3 *Crystal data for dichromate structures*

Compound	$(V/Z)^a$/Å^3	$p_{Cr^{6+}}$ [b]	$p_{O'}$ [c]	∠X—O′—X[d]/°	*Ref*[e].
α-$Na_2Cr_2O_7$	165	5.94, 6.30	2.13	135	54
β-$Na_2Cr_2O_7$	160	6.00, 5.99	2.05	131	55
		6.03, 6.01	2.01	131	
$K_2Cr_2O_7$ ($P2_1/c$)	178	5.08	2.50	145	21
$K_2Cr_2O_7$ ($P\bar{1}$)	181	6.01, 6.02	2.06	124	18, 6, 17, 19
		5.96, 5.99	2.07	128	
$Rb_2Cr_2O_7$ ($P\bar{1}$)	198	6.20, 5.90	2.05	123	23
		6.08, 6.29	2.04	138	
$Rb_2Cr_2O_7$ ($P2_1/n$)	200	6.25, 6.23	1.97	123	22
$Rb_2Cr_2O_7$ ($C2/c$)	195	5.98	2.10	123	15
$SrCr_2O_7$	148	6.20	2.50	133	52
		6.59	2.36	140	
$(NH_4)_2Cr_2O_7$	193	5.95	2.06	121	26
$NaRbCr_2O_7$	181	6.26, 6.03	2.16	136	65
		6.06, 6.17	2.20	141	

[a] V = unit-cell volume /Å^3; Z = formula weights per unit cell;
[b] $p_{Cr^{6+}}$ = bond-strength sum around Cr atom:
$p_{Cr^{6+}} = \sum s_{Cr^{6+}} = \sum\{1.5[r(Cr—O)/1.648]^{-4.9}$;
[c] $p_{O'}$ = bond-strength sum around O′ atom:
$p_{O'} = \sum s_{O'}$
[d] ∠ X—O′—X = bridge angle; [e] Data refer to that of the first reference.

Table 4 *Crystal data for pyrophosphate structures*

Compound	(V/Z)/Å^3	$p_P{}^{5+}$ [a]	$p_O{}'$	∠X—O′—X/°	*Ref.*
α-$Mg_2P_2O_7$	120	5.07 4.95	2.23	144	86, 85
β-$Mg_2P_2O_7$	118	5.02	2.38	180	76, 75
α-$Ca_2P_2O_7$	144	5.04 4.99	2.20	130	31
β-$Ca_2P_2O_7$	135	4.87 4.99	2.08	131	38
		4.97 4.93	2.17	138	
α-$Sr_2P_2O_7$	158	5.14 5.14	2.19	131	33, 32
$Mn_2P_2O_7$	126	5.18	2.32	180	77
$Co_2P_2O_7$	120	4.98 5.06	2.26	143	93
α-$Ni_2P_2O_7$	117	4.83 4.80	2.18	137	87
β-$Ni_2P_2O_7$	116	5.26	2.52	180	78
α-$Cu_2P_2O_7$	120	4.97	2.30	157	84, 83
β-$Cu_2P_2O_7$	120	5.20	2.45	180	79
α-$Zn_2P_2O_7$	121	4.87	2.18	139	88
		5.03 5.01	2.26	148	
β-$Zn_2P_2O_7$	119	4.75	2.32	180	80
$Cd_2P_2O_7$	135	4.99 4.93	2.08	132	27
ZrP_2O_7	138	4.96	2.36	180	111, 112, 113
SiP_2O_7 (AIII)	110	5.09 5.11	2.23	139	116
SiP_2O_7 (AIV)	108	5.42 5.30	2.22	132	117
$Na_4P_2O_7$	170	4.95 4.92	2.04	128	59
$KAlP_2O_7$	136	4.99 5.16	2.15	123	92

[a] $p_P{}^{5+} = \sum \{1.25[r(\text{P—O})/1.534]^{-3.2}\}$; for other symbols see key to Table 3

Reasons for such large deviations are not immediately clear but may be due to next-nearest-neighbour interactions. Mean values of $p_{O'}$ for $Si_2O_7{}^{6-}$, $V_2O_7{}^{4-}$, $Cr_2O_7{}^{2-}$, and $P_2O_7{}^{4-}$, are respectively 1.84, 1.99, 2.11 and 2.24, reflecting the increasing power* of the central ion to polarize the X—O′—X bridge. Data for other miscellaneous pyro-compounds are given in Table 7.

* Using z^2/r, the polarizing powers of $^{IV}Si^{4+}$, $^{IV}V^{5+}$, $^{IV}Cr^{6+}$, and $^{IV}P^{5+}$ are, respectively, 0.6, 0.7, 1.2, and 1.5.

Table 5 *Crystal data for pyrosilicate structures*

Compound	(V/Z)/Å^3	$p_{Si^{4+}}$[a]	$p_{O'}$	∠X—O′—X/°	*Ref.*
$Sc_2Si_2O_7$	127	4.04	2.10	180	5, 68
y-$Y_2Si_2O_7$	141	3.72 3.95	1.84	134	56
D-$Y_2Si_2O_7$	138	4.05	1.86	180	110
A-$Pr_2Si_2O_7$	141	3.89 3.90	1.79	129	34, 35
		4.00 3.90	1.87	133	
G-$Pr_2Si_2O_7$	152	4.20 4.02	2.03	132	34, 35
$Nd_2Si_2O_7$	152	4.05 3.94	2.07	133	37
$Sm_2Si_2O_7$	137	4.00 3.91	1.87	130	39
		4.03 4.12	1.91	136	
$Eu_2Si_2O_7$	147	4.09 3.97	1.76	158	34, 35
$Gd_2Si_2O_7$	147	4.00 3.96	1.76	159	37
$Er_2Si_2O_7$	140	4.05	1.96	180	37
$Yb_2Si_2O_7$	139	3.99	1.96	180	37, 70
$Pb_3Si_2O_7$	191	3.88	1.78	125	121
$Li_6Si_2O_7$	145	3.86	1.68	136	53
$Na_2Mn_2Si_2O_7$	161	3.71 4.08	1.61	127	124
$Na_2ZrSi_2O_7$	151	3.95 3.60	1.73	128	122
$K_2ZrSi_2O_7$	170	4.01 4.04	1.75	148	123
$Na_2Zn_2Si_2O_7$	167	3.84	1.72	132	61
$Na_3ScSi_2O_7$	164	3.93	1.72	136	60
$MnPb_8(Si_2O_7)_3$	617	3.82	1.68	133	120
melilites	152	3.92	1.84	137	46, 42—47

[a] $p_{Si^{4+}} = \sum \{1.0[r(Si—O)/1.625]^{-4.5}\}$; for other symbols see key to Table 3

B. Bond Angles.—The magnitude of the X—O′—X bridge angle in pyro-compounds has also been the subject of several theoretical studies. The first quantitative relationships were given for $Si_2O_7^{6-}$, $P_2O_7^{4-}$, and $S_2O_7^{2-}$ by Cruickshank,[141] who argued that since the bridging oxygen atom has two

[141] D. W. J. Cruickshank, *J. Chem. Soc.*, 1961, 5486.

Table 6 *Crystal data for pyrovanadate structures*

Compound	$(V/Z)/Å^3$	$p_{V^{5+}}$[a]	$p_{O'}$	∠X—O′—X/°	*Ref.*
$Mg_2V_2O_7$	132	5.20	1.95	141	107
		5.02			
β-$Sr_2V_2O_7$	160	5.12	1.89	123	40
		4.96			
		4.89	1.92	124	
		4.82			
$Mn_2V_2O_7$	141	5.13	2.18	180	81
$Co_2V_2O_7$	129	4.88	1.71	118	14
		4.81			
$Ni_2V_2O_7$	125	4.94	1.71	117	14
		4.82			
α-$Cu_2V_2O_7$	140	5.11	2.30	148	104, 103
β-$Cu_2V_2O_7$	145	5.09	2.12	180	90
α-$Zn_2V_2O_7$	145	5.01	2.10	149	89
$Cd_2V_2O_7$	156	4.98	2.16	180	72
$Pb_2V_2O_7$	164	4.97	1.86	122	29, 28
		4.90			

[a] $p_{V^{5+}} = \sum \{1.25[r(V—O)/1.714]^{-5.1}\}$; for other symbols see key to Table 3

Table 7 *Crystal data for miscellaneous pyro-structures*

Compound	$(V/Z)/Å^3$	p_X[a]	p_O	∠X—O′—X/°	*Ref.*
$Y_2SiBe_2O_7$	126	2.08	1.24	129	48
$Er_2Ge_2O_7$	142	4.01	1.96	136	66
$K_2S_2O_7$	164	5.81	1.90	124	30
$Mg_2As_2O_7$	129	5.25	2.56	180	73, 74
$Na_4As_2O_7$	185	4.95	1.96	124	58

[a] $p_{Be^{2+}} = \sum \{0.5[r(Be—O)/1.639]^{-4.3}\}$;
$p_{Ge^{4+}} = \sum \{1.0[r(Ge—O)/1.750]^{-5.4}\}$;
$p_{S^{6+}} = \sum \{1.5[r(S—O)/1.466]^{-4.0}\}$;
$p_{As^{5+}} = \sum \{1.25[r(As—O)/1.681]^{-4.1}\}$; for other symbols see key to Table 3.

p-orbitals available for π-bonding with X atoms, the X—O′—X bonds in a linear (180°) bridge should be shorter and stronger than those in a non-linear bridge. Concomitantly, the non-bridging bonds to X should become longer and weaker as the bridge angle increases. Thus a direct correlation (i) between *d*(X—O′) and X—O′—X angle and (ii) between [*d*(X—O′) − *d*(X—O)] and X—O′—X angle was predicted. From the data available at that time Cruickshank[141] estimated that in isolated $Si_2O_7^{6-}$ and $P_2O_7^{4-}$ pyroanions the bond lengths and bond angles should take the values shown in Table 8. Verification of these values is readily achieved, for example in α-$Mg_2P_2O_7$[86] the P—O′—P

Table 8 *Predicted bond lengths and bridge angles for pyrosilicate and pyrophosphate anions (after Cruickshank*[141]*)*

Anion	*Bridge angle*/°	$(X—O')_{bridge}$/pm	$(X—O)_{terminal}$/pm
$Si_2O_7^{6-}$	180	166	162
	120	170	156
$P_2O_7^{4-}$	180	158	153
	120	164	151

angle is 144° and the mean bond lengths P—O'_{bridge} and P—$O_{terminal}$ are, respectively, 159.1 and 151.6 pm, and in α-$Cu_2P_2O_7$,[84] with angle P—O′—P = 157°, P—O'_{bridge} and P—$O_{terminal}$ are, respectively, 157.6 and 152.5 pm. The correlation (ii) above has been verified in the cases of $Si_2O_7^{6-}$,[136] $P_2O_7^{4-}$,[118] and $V_2O_7^{4-}$,[104] although in each case the correlation is poor. Baur[136] estimates a correlation coefficient of −0.72 for the pyrosilicates but considers the relationship to be a corollary of the [d(Si—O) − ⟨d(SiO)⟩] *versus* $\Delta p_{O'}$ relationship.

Brown and Shannon[137] have similarly noted that the bond strength around the bridging oxygen atom in the pyrophosphates increases with increase in bridging angle. This is shown as a plot of X—O′—X angle against $p_{O'}$ in Figure 9, the data for individual compounds being given in Tables 3—7. Brown and Shannon[137] interpret the large bond-strength sums around O′ in $P_2O_7^{4-}$ ions containing linear (180°) bridges as an effect of the large thermal parameters of O′. These

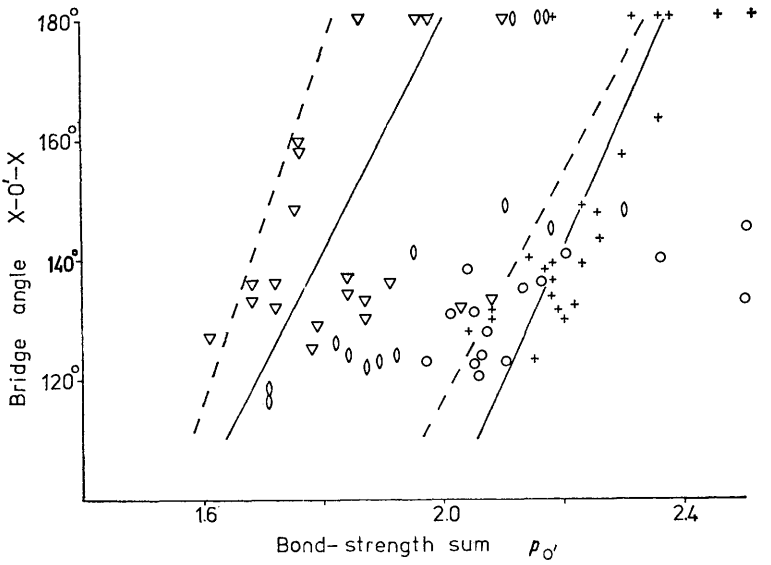

Figure 9 *Plot of* X—O′—X *bridging angle* vs. *bond-strength sum* $p_{O'}$. ▽ = $Si_2O_7^{6-}$; + = $P_2O_7^{4-}$; ○ = $V_2O_7^{4-}$; 0 = $Cr_2O_7^{2-}$.

indicate that the O′ atoms normally disorder from the linear position and that the true P—O′ bond lengths are longer than the observed values. However, no interpretation of the general increase in $p_{O'}$ with bridge angle was offered.

In Figure 9 the mean increases in bond-strength sums around O′ with increases in bridging angles are shown for $P_2O_7^{4-}$ and $Si_2O_7^{6-}$ ions as full lines. The broken lines in Figure 9 correspond to the predictions of Cruickshank[141] based on the data of Table 8. It can be seen that the observed and predicted data are in reasonable agreement, although, as with the $[d(X—O') - d(X—O)]$ *versus* X—O′—X angle relationship of Baur,[136] the correlation is poor. If, as Cruickshank[141] argues, the degree of $p\pi$–$d\pi$ bonding regulates the relationship between the angular distortion and the bridging bond length in a pyroanion, then both components of the distortion, *i.e.* bridging angles and torsion (or twist) angles, should be considered. As yet, no relationship involving torsion angle has been reported. The available data suggest that the relationship between bridging angle and bond-strength sum at O′ (or with bridging bond length) is more tenuous for the pyrovanadates[104] than for the pyrosilicates and pyrophosphates. This may be due to the perturbing influence of stronger next-nearest-neighbour interactions between V^{5+} ions and the oxygen atoms of neighbouring anions, as a result of the greater affinity of V^{5+} for co-ordination greater than four. Certainly the pyrovanadates seem to show greater structural variety than other pyro-compounds, presumably for this reason; see, for example, the structure of β-$Mg_2V_2O_7$.[107]

Since the bridging angles in dichromate-like structures are normally less than in thortveitite-like structures, and since the structural type adopted by a given pyro-compound $M_a[(X_2O_7)_b]$ is largely governed by the cation radius r(M) (see Figure 1), a relationship between bridging angle and r(M), or some function of r(M), would be expected. Figure 10 is a plot of X—O′—X angle *versus* V/Z (the cell volume per formula weight) for the $M_2(X_2O_7)$ compounds and clearly shows that such a relationship holds. By a numerical coincidence the bridging angle (measured in degrees) is less than V/Z (measured in Å^3) in the dichromate-like structures and exceeds V/Z in the thortveitite-like structures. The points numbered 4 and 7 in Figure 10 are those for $Co_2V_2O_7$ and $Ni_2V_2O_7$, respectively, and clearly occupy the dichromate-like region of the plot. This can be compared with Figure 1, in which $Co_2V_2O_7$ and $Ni_2V_2O_7$ were clearly placed in the thortveitite-like region of the r(X) *versus* r(M) plot. The superior predictive capabilities of a volume plot over a radius plot have been noted for several groups of compounds, *e.g.* garnets,[142] pyrochlores,[143] and spinels.[144] The values of V/Z for the pyrophosphates and pyrovanadates of Cd, Co, and Ni are of particular note and are collected in Table 9. These represent the only cations which form both a dichromate-like and a thortveitite-like pyro-compound for which full structural data are available. The difference in the V/Z value of dichromate-like $Co_2V_2O_7$ and that of thortveitite-like $Co_2P_2O_7$ is 9 Å^3. Similarly,

[142] F. Bertaut and F. Forrat, *Compt. rend.*, 1957, **244**, 96.
[143] F. Brisse and O. Knop, *Canad. J. Chem.*, 1968, **46**, 859.
[144] G. Gattow, *Z. anorg. Chem.*, 1964, **333**, 134.

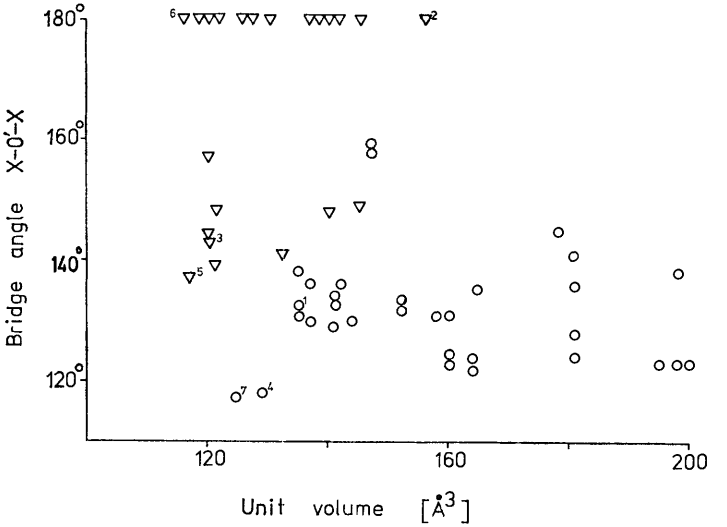

Figure 10 *Plot of* X—O'—X *bridging angle* vs. *the unit volume, V/Z, for the compounds* $M_2(X_2O_7)$. ▽ *indicates thortveitite-like structures;* ○ *indicates dichromate-like structures. Numbered points refer to Table* 9.

Table 9 *Unit volumes of some pyrophosphates and pyrovanadates*

Compound	*(V/Z)*/Å^3	*Structure type*	*Location in Figure 10*
$Cd_2P_2O_7$	135	dichromate-like	1
$Cd_2V_2O_7$	156	thortveitite-like	2
$Co_2P_2O_7$	120	thortveitite-like	3
$Co_2V_2O_7$	129	dichromate-like	4
$Ni_2P_2O_7$	α-116	thortveitite-like	5
	β-117		6
$Ni_2V_2O_7$	125	dichromate-like	7

for $Ni_2V_2O_7$ and $Ni_2P_2O_7$, $\Delta(V/Z)$ is 9 Å^3, which therefore represents the volume difference between $V_2O_7^{4-}$ and $P_2O_7^{4-}$. However, in the case of the Cd^{2+} compounds, the V/Z of thortveitite-like $Cd_2V_2O_7$ exceeds that of dichromate-like $Cd_2P_2O_7$ by 21 Å^3, and this seems to indicate that dichromate-like structures can achieve more efficient packings of $X_2O_7^{n-}$ ions than can thortveitite-like structures. It has been noted previously[72,73] that the observed *a*-axes of thortveitite structures are approximately 25% longer than predicted from an ideally close-packed arrangement, resulting in an inefficient packing which the data of Table 9 support. Concomitant with an inefficient packing of their pyroanions, thortveitite structures invariably show high thermal vibration in their bridging oxygen atoms. It would therefore seem possible that these high thermal parameters result from an attempt by the bridging oxygen atom to occupy the available space more efficiently.